

Robust and predictive fuzzy key performance indicators for condition-based treatment of squats in railway infrastructures

Jamshidi, Ali; Núñez, Alfredo; Dollevoet, Rolf; Li, Zili

DOI

[10.1061/\(ASCE\)IS.1943-555X.0000357](https://doi.org/10.1061/(ASCE)IS.1943-555X.0000357)

Publication date

2017

Document Version

Accepted author manuscript

Published in

Journal of Infrastructure Systems

Citation (APA)

Jamshidi, A., Núñez, A., Dollevoet, R., & Li, Z. (2017). Robust and predictive fuzzy key performance indicators for condition-based treatment of squats in railway infrastructures. *Journal of Infrastructure Systems*, 23(3), Article 04017006. [https://doi.org/10.1061/\(ASCE\)IS.1943-555X.0000357](https://doi.org/10.1061/(ASCE)IS.1943-555X.0000357)

Important note

To cite this publication, please use the final published version (if applicable). Please check the document version above.

Copyright

Other than for strictly personal use, it is not permitted to download, forward or distribute the text or part of it, without the consent of the author(s) and/or copyright holder(s), unless the work is under an open content license such as Creative Commons.

Takedown policy

Please contact us and provide details if you believe this document breaches copyrights. We will remove access to the work immediately and investigate your claim.

1 **Robust and Predictive Fuzzy Key Performance Indicators for Condition-** 2 **Based Treatment of Squats in Railway Infrastructures**

3 Ali Jamshidi, Section of Railway Engineering, Delft University of Technology, The Netherlands.
4 Alfredo Núñez, Section of Railway Engineering, Delft University of Technology, The Netherlands.
5 Rolf Dollevoet, Section of Railway Engineering, Delft University of Technology, The Netherlands.
6 Zili Li, Section of Railway Engineering, Delft University of Technology, The Netherlands.
7 A.Jamshidi@tudelft.nl, A.A.NunezVicencio@tudelft.nl, Z.Li@tudelft.nl, R.P.B.J.Dollevoet@tudelft.nl
8

9 **ABSTRACT**

10 This paper presents a condition-based treatment methodology for a type of rail surface defect called "squat".
11 The proposed methodology is based on a set of robust and predictive fuzzy key performance indicators. A
12 fuzzy Takagi Sugeno interval model is used to predict squat evolution for different scenarios over a time
13 horizon. Models including the effects of maintenance to treat squats, via either grinding or replacement of
14 the rail, are also described. A railway track may contain a huge number of squats distributed in the rail
15 surface with different levels of severity. We propose to aggregate the local squat interval models into track-
16 level performance indicators including the number and density of squats per track partition. To facilitate the
17 analysis of the overall condition, we propose a single fuzzy global performance indicator per track partition
18 based on a fuzzy expert system that combines all the scenarios and predictions over time. The proposed
19 methodology relies on the early detection of squats using Axle Box Acceleration measurements. We use real-
20 life measurements from the track Meppel-Leeuwarden in the Dutch railway network to show the benefits of
21 the proposed methodology. The use of robust and predictive fuzzy performance indicators facilitates the
22 visualization of the track health condition and eases the maintenance decision process.

23
24 **Keywords:** Design of key performance indicators, railway track condition monitoring and maintenance,
25 interval fuzzy models.

27 INTRODUCTION

28 During the recent years, a modal shift from road to rail has been promoted in Europe. The idea is to increase
29 the share of transport demand for mobility of people and freight. Reduce road traffic congestion, make
30 efficient use of the energy resources and tackle the major challenges of climate change. Major contributions
31 are needed in the optimal management of railway assets, evolving towards a more automated predictive
32 operation where functional assets are monitored. This includes all the important indicators such as
33 economical, safety and societal impacts, considering the perspective of both railway infrastructure manager
34 and users (Zoeteman 2001).

35

36 A typical set of railway assets is shown in Figure 1, and it includes the track, station, superstructure, sub-
37 structure, communication, catenary, control room, signalling system, rolling stock, barrier, security and
38 surrounding. In order to monitor and properly maintain the railway assets, it is necessary to measure the
39 evolution of important health condition indicators over time, also called key performance indicators (KPIs),
40 for each of the critical assets. For example, in the Figure 1, $J_{label}^{Asset}(t)$ relates to the KPI for the health condition
41 of an asset called "Asset", uniquely labelled as "label" at time t . In The Netherlands, the assets in the railway
42 network includes more than 3,000 km of track, 388 stations, being one of the densest networks in Europe. In
43 this network, the design of an optimal maintenance plan for all its assets is a challenging problem. To
44 optimally design the maintenance plans, infrastructure manager requires to provide crucial information of
45 each asset (Stenström et al. 2015), and maintenance decision making considering risk averse situations
46 (Rockafellar and Royset 2015). Thus, the optimal maintenance plan is a necessity because of the high
47 demand from users and government for a better quality of service, and the need of keeping costs as low as
48 possible.

49 Maintenance Performance Indicators evaluate the system performance and can be used to guarantee that
50 these assets operate at an acceptable level of functionality and safety. In Parida and Chattopadhyay (2007), a

51 general systems framework is proposed using a hierarchical structure of multicriteria maintenance
 52 performance measurements. In Ahren and Parida (2009), the same framework is applied to the case of
 53 benchmarking railway infrastructures maintenance operations. Three different hierarchical levels are
 54 proposed: strategic level for top management decisions, tactical level for middle management and functional
 55 level for supervisors/operators. The general framework requires effective measurements of the health
 56 condition of the assets considering that the different assets degrade with different rates due to the effect of
 57 different exogenous sources. Particularly, the focus of this paper is to design robust and predictive fuzzy
 58 performance indicators for health condition monitoring of railway tracks, considering a particular major type
 59 of Rolling Contact Fatigue (RCF) called squat (see Li et al. 2015).

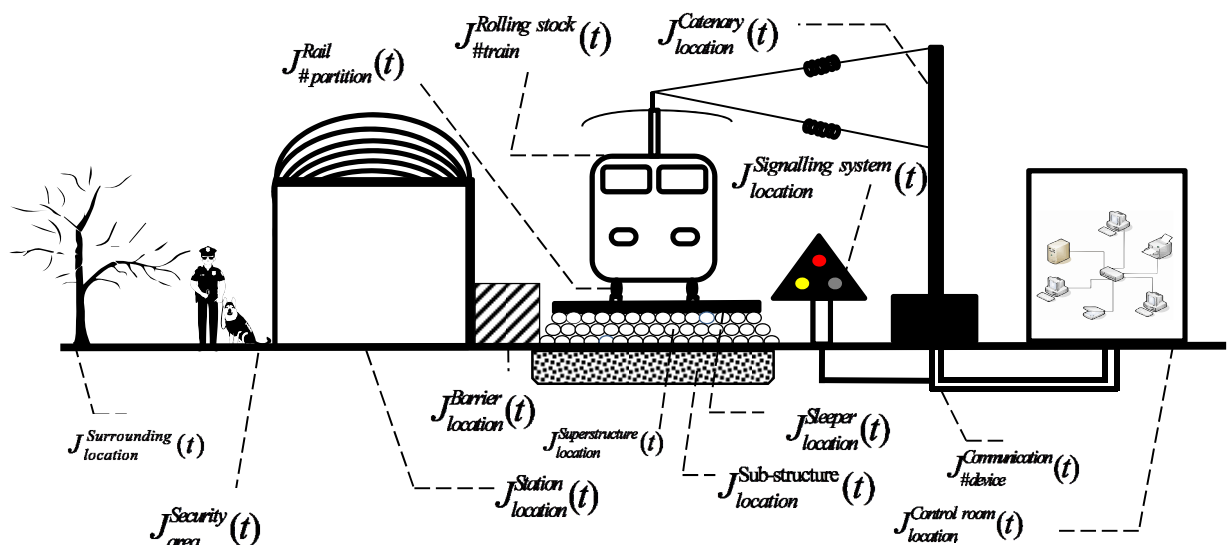


Figure 1: Main components of railway infrastructures.

72 In The Netherlands over forty percent of the railway maintenance budget is allocated yearly to track
 73 maintenance (Zoeteman and van Meer 2006; Zoeteman et al. 2014). The presence of RCFs accelerates track
 74 degradation which negatively influences its health condition. It also increases the noise level that affects

75 people living in the surroundings and in a worst case making a huge impact on safety as severe RCF's can
76 result in derailment. For track maintenance to be effective, the planning should consider not only costs but
77 also the dynamics of RCFs. Complex interactions between environment, vehicles, wheels and track interface,
78 structure and also different behaviours under maintenance operation such as grinding and rail replacement
79 can be considered. In Patra et al. (2009) rail degradation is modelled by a time to failure function using MGT
80 (million gross tons) measurements and around 12 failure events, decision making is proposed in a Monte
81 Carlo simulation setting. The maintenance operations are modelled as different cost functions, including rail
82 grinding costs, track tamping costs, rail lubrication costs, among other maintenance operations. Stenstrom et
83 al., (2015) assess the value of preventive maintenance in comparison with corrective maintenance. The idea
84 is to analyse cost-benefit of using preventive maintenance including four different maintenance costs:
85 maintenance inspections, repair of potential failures, repair of functional failures and service/production loss.
86 In the case study for a Swedish railway line, the ten costliest railway sections are found to have three times
87 the tonnage compared to the sections with the lowest costs, and also the costliest sections experience 4.5
88 times more track failures. The conclusion is that the railway sections with the lowest total maintenance cost
89 have implemented more preventive maintenance actions.

90
91 In the literature, different studies have been carried out to present how a degradation model for tracks can
92 be embedded on asset management to facilitate maintenance plans. Track geometry measurements relying
93 on statistical analysis are used to capture the track degradation effect (Sadeghi and Askarinejad 2010;
94 Andrade and Teixeira 2011; Andrews 2012; Andrade and Teixeira 2012; Vale and Lurdes 2013; Nathanail
95 2014; Guler 2014; Weston et al., 2015). In those papers, different time-dependent degradation models are
96 proposed, they can all be used to improve maintenance interventions. Estimation of the track safety and
97 considering the probability of rail break has also been investigated (Schafer and Barkan 2008; Burstow et al.
98 2002; Sandstrom and Ekberg 2009). Detailed mechanical models can give many insights about the evolution

99 of rail defects; however, the use of those models for maintenance planning operations require sophisticated
100 knowledge about the track and its operational conditions that are not always available or easy to obtain in
101 practice. Fuzzy logic has increasingly been used in different fields; in particular, in the ones where
102 uncertainties can influence the decision process. It is used to measure performance in different
103 infrastructures by predicting failure of components (Senouci et.al 2014; Sadiq et al. 2004), optimizing asset
104 condition (Xu et al. 2014; Wang and Liu 1997) and decision making (Khatri et al. 2011). In this paper, we
105 propose the use of interval fuzzy model to capture the most important dynamics of squats in railway
106 infrastructure, from the maintenance operation point of view. We aim to keep the prediction as simple as
107 possible, but suitable enough to ease decision making in practice. The use of key performance indicators
108 (KPIs) that are able to explicitly include the dynamics of the deterioration of the assets, together with an
109 appropriate set of scenarios for the principal sources of stochasticities that might affect their performance
110 are recommended. A fuzzy Takagi Sugeno (TS) interval model (Škrjanc, 2011; Núñez and De Schutter, 2012;
111 Sáez et al., 2015) is calibrated using real-life data collected over years of field test and measurements. That
112 helps obtaining numerical models capable to predict squat growth over a time horizon under different
113 possible scenarios and under different maintenance decisions.

114
115 Based on the interval fuzzy models for squats, a condition-based methodology for rails is proposed using
116 different KPIs that are defined in a track-partition level which allows the grouping of defects located in a
117 given track partition. In this methodology, number and density of squats are considered over a prediction
118 horizon under three different scenarios, vis. slow, average and fast growth. Then, to facilitate visualization of
119 the track health condition and to ease the maintenance decision process, we propose a fuzzy global KPI
120 based on fuzzy rules for each partition that merges the different KPIs over prediction horizon and scenarios.
121 The methodology is evaluated with data from a Dutch railway track, relying on the use of technology based
122 Axle Box Acceleration (ABA) measurements, capable to detect the early stage squats on the rail (Molodova et

123 al. 2014, Li et al. 2015). An introduction of the ABA measuring system is described in ABA based health
124 condition monitoring in railways, including background of the ABA measurement system and its application
125 in rail condition monitoring based on ABA.

126
127 Figure 2 shows the flowchart of the proposed methodology divided in three steps. In Step 1, relying on ABA
128 measurements, the health condition of the track and severity are estimated. A list of defects is assumed to
129 be provided by the detection algorithm. In Step 2, using interval fuzzy TS model, the growth of each detected
130 defect i is evaluated over time and different possible evolution scenarios are considered. Three models are
131 evaluated, with grinding, replacement and without maintenance. The idea is to see the consequences of the
132 maintenance operations on the detected squats for different scenarios over a prediction horizon. At the end,
133 in Step 3, a global fuzzy KPI is used to describe the condition at a track partition level, for a given travel
134 direction, left and right rails. The global fuzzy KPI at a partition, combines the effects of a vector of KPIs over
135 a prediction horizon, considering three most representative defect evolution scenarios.

136
137 The paper is divided as follows. In next section, the main elements of the ABA based detection methods are
138 presented. Next, fuzzy interval models for squats are presented for three cases: without maintenance, after
139 grinding and after replacement. After, different KPIs are defined at a track partition level in order to
140 aggregate the local dynamic behaviour of squats. Because of the number of scenarios and prediction horizon,
141 the fuzzy global KPI is proposed to facilitate decision making. Later, the numerical results and discussion are
142 presented. Finally conclusions and further research are discussed.

143
144
145
146

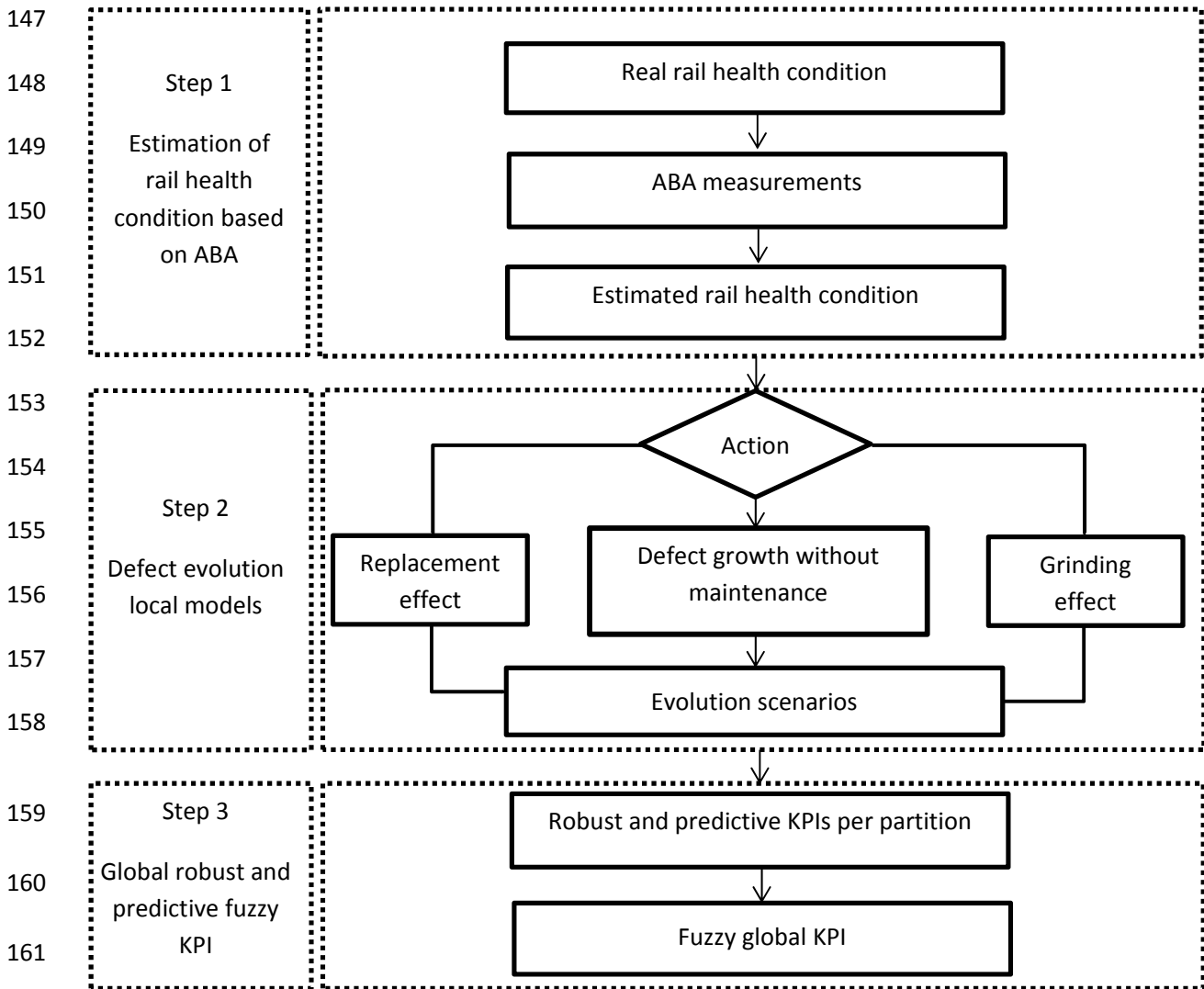


Figure 2: flowchart of the proposed methodology

ABA BASED HEALTH CONDITION MONITORING IN RAILWAYS

a. BACKGROUND OF THE ABA MEASUREMENT SYSTEM

There are different methods to diagnose the condition of rail defects, including ultrasonic measurements, eddy current testing, image recognition and guided-wave based monitoring among other technologies. Each of them has different advantages and disadvantages. In this paper, we need a technology capable to detect defects in an early stage, thus we consider the use of ABA measurements (Li et al. 2008; Molodova et al.

170 2014). Li et al. (2015) investigated the feasibility of detecting early-stage squats using an ABA prototype. It is
171 reported that squats could be detected by analysing the frequency content of the ABA signals in the wavelet
172 power spectrum. In practice, the useful frequency band for early detection of squats ranges from 1000-2000
173 Hz and 200-400 Hz (Molodova et al. 2014). In the literature, it has been reported that ABA systems can be
174 employed to detect surface rail defects like corrugation, squats and welds in poor condition. The ABA system
175 offers the advantages of (1) having a lower cost than other types of detection methods, (2) it is easy to
176 maintain and (3) can be implemented in-service operational trains. Other significant advantages that ABA
177 offers over similar measurement systems are (4) the ability to detect small defects with the absence of
178 complicated instrumentation and (5) the ability to indicate the level of the dynamic contact force (Molodova
179 et al. 2015).

180

181 **b. RAIL CONDITION MONITORING BASED ON ABA**

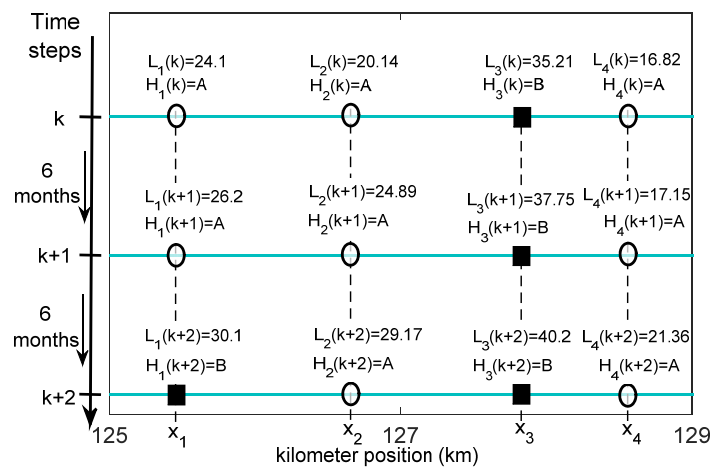
182 In this study, we are users of the ABA detection methodology presented in Li et al. (2015) and Molodova et
183 al. (2014); thus, we assumed that a list of squats and their location are available. Let's define the counter of
184 squat defects as $i=1,2,\dots,N_{defects}$, where x_i represents the position of the squat i . We define $H(x,k)$ and $L(x,k)$ as
185 the real rail condition and real squat length respectively, defined at position x and time step k . We only focus
186 on positions x_i where squats are detected. To simplify the notation, we assume $H_i(k)=H(x_i,k)$ and $L_i(k)=L(x_i,k)$
187 represent the severity and the length of squat i at time step k .

188 To systematically classify squats in terms of severity, we follow the terminology used in Smulders (2003), UIC
189 Code (2002) and Rail Damages (2001). The definitions of these three references are compatible to one
190 another. Although the transition between one class to the other is not always abrupt, we have defined fixed
191 values for those transitions according to our experience. Depending on the squat length $L_i(k)$, measured in
192 mm, the severity of the squat can be used to represent the health condition of the rail at location x_i as
193 follows:

194

$$H_i(k) = \begin{cases} S & \text{if } 0 \leq L_i(k) < 8 \\ A & \text{if } 8 \leq L_i(k) < 30 \\ B & \text{if } 30 \leq L_i(k) < 50 \\ C & \text{if } 50 \leq L_i(k) < 60 \\ RC & \text{if } L_i(k) \geq 60 \end{cases} \quad (1)$$

195 where *S* refers to a seed squat, *A* is a light squat (*A* squat), *B* is a moderate squat (*B* squat), *C* is a severe squat
 196 (*C* squat) and *RC* is a squat with risk of derailment. The boundaries were defined based on general guidelines
 197 to classify squats. Figure 3 depicts an example of defects growths collected from field measurements in the
 198 track Meppel-Leeuwarden. In the figure, x-axis represents kilometre position of the track where the squats
 199 are located and y-axis indicates time in three different months, month 0 (moment of the measurement),
 200 month 6 and month 12. In the diagram, *A* squats are drawn as circles and *B* squats are squares. Different
 201 squats grow with different rates. In the average case, the track measurements show that it takes
 202 approximately 9 months for a *A* squat of 20 mm to evolve into a *B* squat of 30 mm.



203

204 Figure 3: An example of defects evolution over time. The x axis is the kilometre position in the track, x_i the
 205 position of squat i , y axis is time every six months. In circles are *A* squats, squares are *B* squats.

206 In this study, the ABA measurements are used to develop a model for defect evolution. For each squat, the
 207 related energy of the ABA is available using wavelet spectrum analysis and advanced signal processing

208 methods (Molodova et al. 2014). Relying on the ABA measurement, the energy values of the ABA signals can
 209 be calculated at every position x at time step k as $E(x,k)$. From the energy signal, we are interested only in
 210 those locations with squats, namely $E_i(k)=E(x_i,k)$. For using the energy of the ABA signal to predict the squat
 211 length evolution, a correlation between the squat length and energy of the ABA signal was performed.
 212 Photographs from track visits of several years are used to measure the lengths of the squats and to fit the
 213 piecewise linear correlation model. The estimated length $\hat{L}_i(k)$ of squat i at time step k as function of the
 214 energy value $E_i(k)$ is given by:

$$215 \quad \hat{L}_i(k) = \begin{cases} g_1 E_i(k) + q_1 & \text{if } E_i(k) < 80 \\ g_2 E_i(k) + q_2 & \text{if } 80 \leq E_i(k) < 170 \\ g_3 E_i(k) + q_3 & \text{if } 170 \leq E_i(k) < 300 \\ g_4 E_i(k) + q_4 & \text{if } E_i(k) \geq 300 \end{cases} \quad (2)$$

216 where the slope of local linear functions is g_m , $m=1,\dots,4$, and the bias q_m , $m=1,\dots,4$, are adjusted to the
 217 specific track. For relation (2), we have been users of previous work of our group, Li et al. 2011, Li et al. 2015,
 218 Molodova et al. 2015. In general, we can say that the correlation coefficient and residual standard get
 219 affected by the speed of the measurement train. In this paper, we assumed that the measurement is done at
 220 commercial speed as was done for the test measurement so far, and we have disregard segments that were
 221 measured out of a reasonable range of speed.

222 A global view of the Step 1 of the methodology, estimation of track health condition based on ABA, is
 223 presented in Figure 4. As shown in the figure, in order to estimate length $L_i(k)$, the energy value $E_i(k)$ is
 224 calculated using the ABA measurement. Hence, relying on the estimated squat lengths, the rail health
 225 condition $H_i(k)$ can be approximated. In the figure, a squat is detected with an energy value $E_i(k)=145 \text{ m}^2/\text{s}^4$,
 226 the estimated squat length $\hat{L}_i(k) = 43 \text{ mm}$ and the estimated health condition $\hat{H}_i(k) = B$.

227

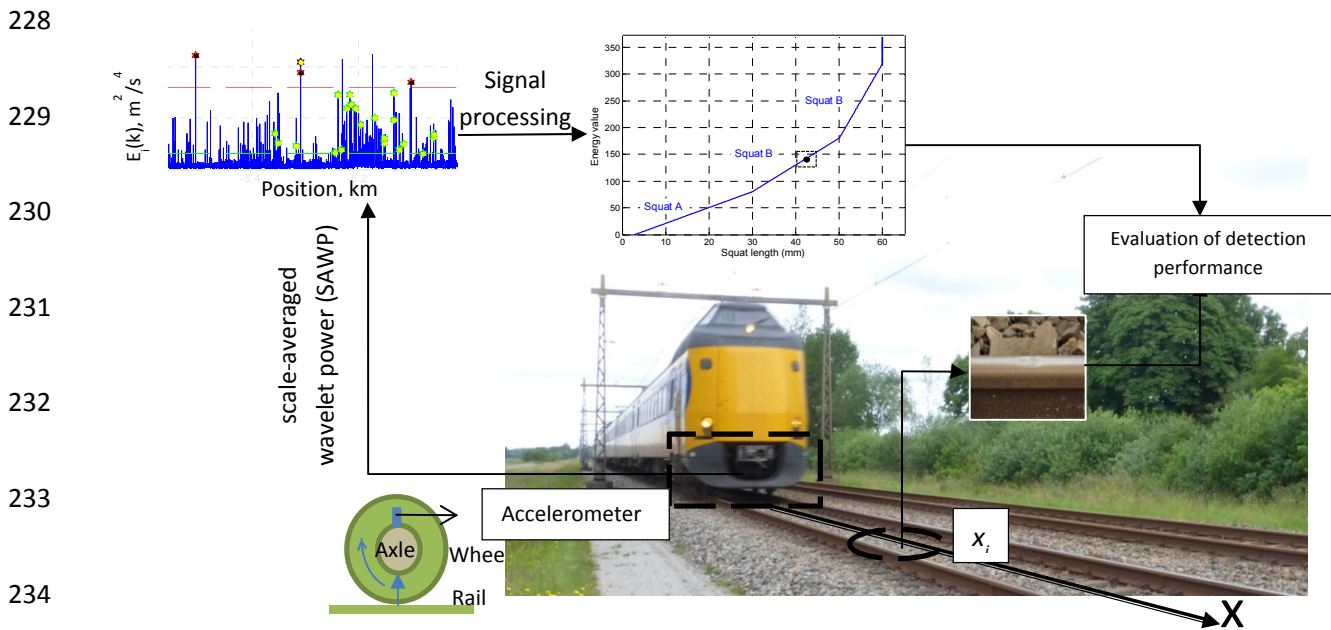


Figure 4: Global scheme of the main components of the Step 1: Estimation of track health condition based on ABA

FUZZY INTERVAL MODELS FOR SQUATS

a. MAINTENANCE ORIENTED MODELS FOR SQUATS

Typically, maintenance slots in the Dutch railway network are decided based on long and short term planning for preventive and corrective maintenance respectively. In the long term, the contractor should inform asset manager at least one year before cyclic grinding for using the equipment needed. In the short term, normally, the maintenance is performed when the squats are in the last stage of growth (C squat). Thus, a predictive approach by employing well designed KPIs should aim to improve both short and long term planning, (1) keeping a good balance between costs and health condition of the track, (2) simplify the design of maintenance plan over the whole time horizon and (3) increase indirectly the track safety.

248 The experimental results show that each squat can grow with different rates. The estimation of squat lengths
249 can be affected by the subjectivity of the human error. For instance, one source of uncertainty comes from
250 the fact that visually only the rusty area of the defects is used to measure length, while the defect might be
251 longer. Fuzzy systems can work under subjective environments. In the proposed methodology, the design of
252 the global fuzzy KPI deals with the subjectivity. The definition of a low or a big number of defects will depend
253 on the subjectivity of the inframanager, and on how this information is incorporated for maintenance
254 decision making. In order to generalize this characteristic, fuzzy confidence intervals can be used to capture
255 the stochasticities of different scenarios for the squat growth. The upper bound of the interval represents a
256 worst case scenario, while the lower bound represents a slow rate grow scenario. In the fuzzy interval
257 approach, the average behaviour is given by a Takagi-Sugeno (TS) fuzzy model. This is used to approximate
258 nonlinearities by smoothly interpolating affine local models. Each local model is involved in the global model
259 based on the activation of a membership function. According to literature, the identification of fuzzy interval
260 models is divided on three steps: clustering method to generate fuzzy rules, identification of the TS local
261 linear parameters (average model), and identification of the fuzzy variance for each rule (Škrjanc et al. 2004;
262 Škrjanc 2011). In this paper, we use the fuzzy interval approach proposed in Nunez and De Schutter (2012)
263 and Sáez et al. (2015), which includes Gustafson Kessel clustering, local identification of the linear
264 parameters and optimization of a parameter α to adjust the width of the interval, minimizing both area of
265 the band and number of data points outside the band.

266
267 The general problem of interval defect evolution is as follows. Let's consider different defect growth
268 scenarios $h = h_1, h_2, \dots, h_H$, time steps $t = k, k + 1, k + 2, \dots, k + N_p$, and $u(k)$ the maintenance action at
269 time step k . The prediction model for the growth of a squat can be written as:

$$270 \quad \hat{L}_i^h(k+1) = f_j^h(L_i(k), u(k)), \quad x_i \in [x_j, x_{j+1}] \quad (3)$$

271 where $\hat{L}_i^h(k+1)$ is an estimation of length of the squat i located in the track partition j at the time step $k+1$
 272 considering the scenario h . The model considers the effect of maintenance $u(k)$ and the initial condition of
 273 the squat $L_i(k)$. Depending on the location of the squat i , x_i , we use a local model corresponding to the
 274 track partition j where the squat is located, $x_i \in [x_j, x_{j+1})$. We assume the dynamics for different squats are
 275 similar if they are in the same track partition under the same scenario.
 276 In this paper, three maintenance actions are considered, $u(k) = \{u_1, u_2, u_3\}$, where u_1 is without
 277 maintenance, u_2 is grinding and u_3 is replacement. Also three scenarios are evaluated, $h = h_1, h_2, h_3$, where
 278 h_1 represents slow growth, h_2 average growth and h_3 is fast growth scenarios.

279

280 b. DYNAMICS OF SQUATS WITHOUT MAINTENANCE

281 In the absence of maintenance, $u(k) = u_1$, the prediction model for the average growth scenario, h_2 , is
 282 formulated based on TS fuzzy model:

283

$$284 \quad \hat{L}_i^{h_2}(k+1) = f_j^{h_2}(L_i(k), u_1) = f_j^{\text{TS}}(L_i(k)) = \sum_{r=1}^{N_R} \beta_{jr}(L_i(k)) L_{jr}(k), \quad (4)$$

$$285 \quad L_{jr}(k) = a_{jr} L_i(k) + b_{jr}, \quad (5)$$

$$286 \quad \beta_{jr}(L_i(k)) = \frac{A_{jr}(L_i(k))}{\sum_{r=1}^{N_R} A_{jr}(L_i(k))}, \quad (6)$$

287 where a_{jr}, b_{jr} are the parameters of the fuzzy local model on rule r , $r = 1, 2, \dots, N_R$ and $\beta_{jr}(L_i(k))$ is the
 288 normalized activation degree of the rule r . In this paper we will use Gaussians to model the membership

289 degrees, $A_{jr}(L_i(k)) = \exp\left(-0.5c_{jr,1}\left(L_i(k) - c_{jr,2}\right)^2\right)$, defined by parameters $c_{jr,1}$ and $c_{jr,2}$ given by the
 290 Gustafson Kessel clustering algorithm.

291
 292 Once the TS model is obtained, slow growth scenario and fast growth scenario are used as lower and upper
 293 bound of the average growth scenario, $\hat{L}_i^{h_2}(k+1)$, respectively. The equations can be defined as:

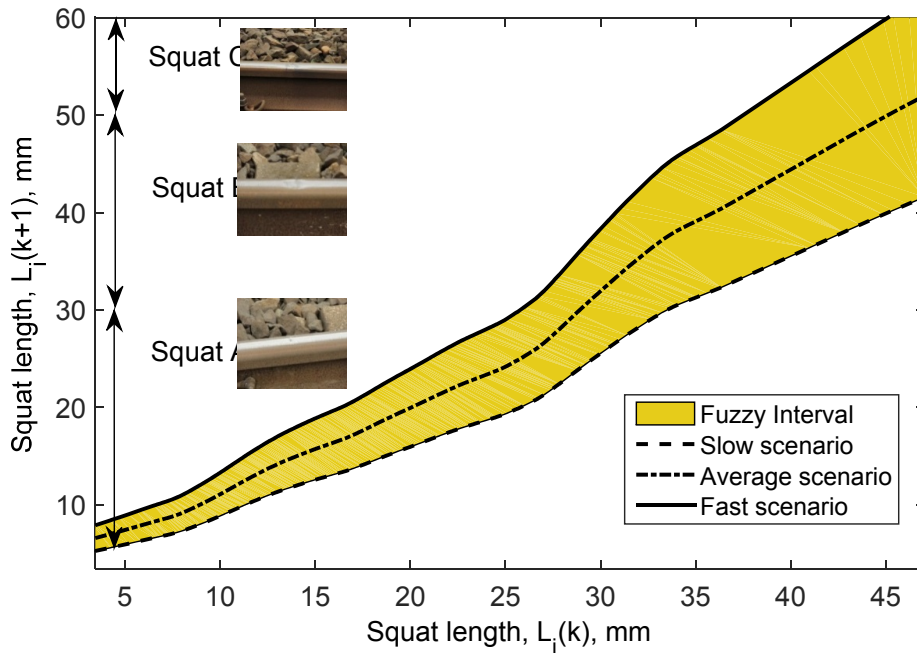
$$295 \quad \hat{L}_i^{h_3}(k+1) = \overline{f}_j^{\text{TS}}(L_i(k)) = \sum_{r=1}^{N_R} \beta_{jr}(L_i(k)) \left(L_{jr}(k) + \alpha^{h_3} \Delta_{jr}(L_i(k)) \right) \quad (7)$$

$$296 \quad \hat{L}_i^{h_1}(k+1) = \underline{f}_j^{\text{TS}}(L_i(k)) = \sum_{r=1}^{N_R} \beta_{jr}(L_i(k)) \left(L_{jr}(k) - \alpha^{h_1} \Delta_{jr}(L_i(k)) \right) \quad (8)$$

$$297 \quad \Delta_{jr}(L_i(k)) = \sigma_{jr} \left(1 + \psi_{jr}^T (\varphi_{jr} \varphi_{jr}^T)^{-1} \psi_{jr} \right)^{0.5} \quad (9)$$

298 where $\hat{L}_i^{h_3}(k+1)$ is the estimated growth length of squat i in time step $k+1$ in fast scenario, and $\hat{L}_i^{h_1}(k+1)$ is
 299 estimated growth length in slow scenario, α^{h_3} and α^{h_1} are tuning parameters in the fast growth scenario
 300 and the slow growth scenario respectively. Moreover, $\varphi_{jr} \varphi_{jr}^T$, $\psi_{jr} = [L_i(k), 1]^T$ and σ_{jr} are covariance
 301 matrix, regression matrix and variance of the local model.

302
 303 Figure 5 depicts the proposed fuzzy confidence interval model including 177 data points used to capture the
 304 squat evolution in different stage of growth. A subset of the data used for analysis is included in Table 1. A
 305 squats from 8 to 30 mm in length have no or shallow cracks. The B squats ranging from 30 to 50 mm grow
 306 quickly. The B squats evolve to C squats when the network of cracks beneath the squat gets further spread. All
 307 three stages are shown by reference photos of A squat, B squat and C squat in Figure 5.



308

309

Figure 5: Interval fuzzy model for squat growth in the case study track.

310

311

312

Table 1: a subset of data used for squat analysis including defect position, km, and visual length, mm, at time k and k+1

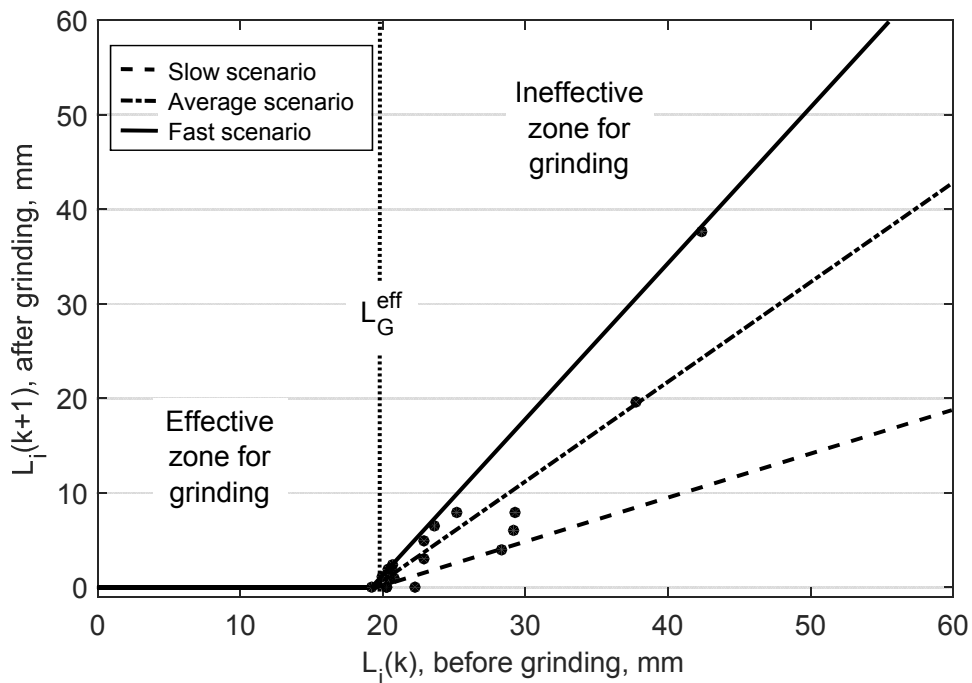
Squat	Position, km	$L_i(k)$, mm	$L_i(k+1)$, mm	Squat	Position, km	$L_i(k)$, mm	$L_i(k+1)$, mm
1	104.8438	30.7260	34.7465	11	105.4613	22.8311	24.6695
2	105.1051	37.7420	40.5086	12	105.4953	19.5933	22.0216
3	105.1404	33.2264	37.0496	13	105.5827	14.5360	16.7962
4	105.2116	34.2207	37.7779	14	105.5852	19.5432	21.9787
5	105.3215	46.7870	49.1017	15	105.6353	11.0032	13.9019
6	105.3901	33.0151	36.8862	16	105.6591	25.1642	27.1955
7	105.4195	19.1797	21.6607	17	105.7462	15.4564	17.7552
8	105.4269	20.2236	22.5435	18	106.3105	28.7262	32.2116
9	105.4344	9.4918	12.4747	19	106.8735	55.1141	57.1707
10	105.4561	33.2798	37.0903	20	107.2845	17.8761	20.4044

313

314 c. RAIL GRINDING EFFECT

315 Squats can be effectively treated by grinding when they are in early stage of growth. Cyclic rail grinding keeps
 316 control of not only maintaining the rail profiles but to plan track maintenance efficiently (Magel and Kalousek
 317 2002). Figure 6 depicts squat growth before and after grinding where black points show those squats that did

318 not disappear after grinding. As seen in the figure, some *A* squats are located in the effective zone of grinding
 319 such that these squats have a zero length after grinding. Those *A* squats that are imminent to become *B* squats
 320 are located in the ineffective zone for grinding as well as *B* squats and *C* squats. Moreover, three growth
 321 scenarios in the effective zone are specified to capture the squat evolution rate. Even though grinding severe
 322 squats postpones rail replacement, it could accelerate squat evolution as the cracks are not totally
 323 disappeared.
 324



325
 326 Figure 6: Squat growth before grinding and after grinding classified in two effective and ineffective zones for
 327 grinding operations. In this case, the depth of the grinding was around 1.0 mm.

328
 329 The growth model for squat *i* by considering grinding effect can be expressed as:
 330

$$\hat{L}_i^h(k+1) = \begin{cases} 0 & L_i(k) \leq L_G^{eff} & \text{Effective zone for grinding} \\ z_G^h(L_i(k) - L_G^{eff}) & L_i(k) > L_G^{eff} & \text{Ineffective zone for grinding} \end{cases} \quad (10)$$

332

333 where L_G^{eff} is the critical squat length that estimate effectivity of grinding, L_G^{eff} is around 20mm in Figure 6

334 for a grinding depth of 1.0 mm, z_G^h is the slope of the linear model in the ineffective zone for grinding for

335 different scenarios h , slow, average and fast growth scenarios.

336

337 **d. RAIL REPLACEMENT EFFECT**

338 When the squat severity becomes worse and cracks are grown considerably, grinding is not efficient

339 anymore. Therefore, replacement is the only solution. As replacing a piece of rail takes time and it is costly,

340 an optimal decision making for when and where the rail should be replaced is important. Higher rail (larger

341 radius) and low rail (smaller radius) have different degradation behaviours (Patra et al. 2009), thus usually

342 only the most needed rail is replaced. Rail replacement is performed using welds to connect the new rail with

343 the old one. After replacement, the rail surface defects will totally disappear by the installation of new rail

344 whereas development of new squats will depend on various factors, like track conditions, MGT, and other

345 different factors. In the case of the welds, because they are composed by materials with different properties

346 than the rails, they are prone to squat defect appearance (Lewis and Olofsson 2009).

347

348 Figure 7.a and 7.b show squat growth before and after rail replacement. Figure 7.a shows the squat growth

349 between welds where all the squats will disappear after replacement. The model assumes that no squats will

350 appear during a long horizon by considering that new developed squats can be detected in the next

351 measurement campaign. Figure 7.b shows squat growth on the welds a period after replacement. The exact

352 time instant when the growth starts is related to quality of the weld. This means that for those welds that

353 have good quality, the starting point would be much later.

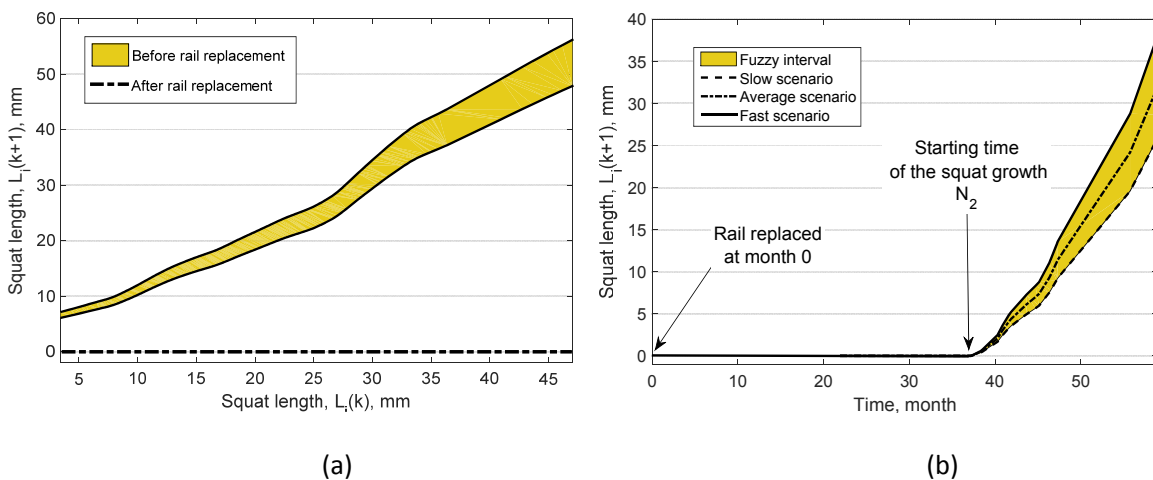
354
 355 In the case of between welds, the squat length after replacement is equivalent to zero during a time horizon
 356 N_1 . The growth model on the weld can be expressed according to the time N_2 , when squat can appear.
 357 Before time $k + N_2$ no squat is present in the weld, while at $k + N_2 + 1$ the squat will start to appear and
 358 evolved based on the proposed growth scenarios.

359
$$\hat{L}_i^h(x_{w_1}, k+t) = 0 \quad t = 1, 2, \dots, N_1, h = h_1, h_2, h_3 \quad (11)$$

360
$$\hat{L}_i^h(x_{w_2}, k+t) = 0 \quad t = 1, 2, \dots, N_2, h = h_1, h_2, h_3 \quad (12)$$

$$\hat{L}_i^h(x_{w_2}, k + N_2 + 1) = \begin{cases} \underline{f}_i^{TS}(\Delta L_i) & \text{if } h = h_1 \\ \underline{f}_i^{TS}(\Delta L_i) & \text{if } h = h_2 \\ \bar{f}_i^{TS}(\Delta L_i) & \text{if } h = h_3 \end{cases}$$

361 where x_{w_1} is some position between the welds, x_{w_2} is the location of the weld, and ΔL_i is small value that
 362 triggers the growth when the squat i starts evolving at the thermite weld at time instant $k + N_2 + 1$. After the
 363 squat appears, the interval fuzzy model will capture its evolution over time.



364
 365 (a) (b)
 366 Figure 7: (a) After rail replacement with a piece of new rail free of damage, the length of squats $L_i(k+1)$ will
 367 become zero no matter their initial length $L_i(k)$; (b) on welds after rail replacement a squat is prone to
 368 appear.

369 **KPIs FOR RAIL HEALTH CONDITION**

370 **KPI DESCRIPTION**

371 The monitoring of the evolution of a single squat might not be practical from the maintenance perspective.
 372 Aggregated information over bigger track partitions can facilitate infrastructure manager decision over the
 373 maintenance plans. In the case of squats, we propose key performance indicators (KPI's) considering the
 374 number of *A*, *B* and *C* squats and the number of squats with potential risk of rail break called *RC* squats, at
 375 different time *t* and different growth scenario *h*. Moreover, as significant number of *B* and *C* squats near to
 376 each other indicate a high potential risk to track safety, a KPI is proposed relying on a measure of density of
 377 squats *B* and *C*. Let's assume the function $\delta_{h,j}^d(x,k)$ is provided by the ABA detection algorithm, for the
 378 current instant of measurement *k*. The function equals to 1 if a squat type $d \in \{A, B, C, RC\}$ is located at
 379 position *x*, instant *k*, partition *j* and growth scenario *h* and equals to zero otherwise. Used as initial condition,
 380 and relying on the interval fuzzy model, it is possible to predict $\delta_{h,j}^d(x,t)$ for any time horizon, $t=1, \dots, N_p$. The
 381 growth of new squats during the prediction horizon is not considered in this work, because we assume that
 382 new squats will be detected in the next measurement campaign at instant *k+1*, where the models can be
 383 updated according to the new conditions. The KPIs of squat numbers at partition *j*, instant *t*, scenario *h*, can
 384 be expressed as:

$$\begin{aligned}
 y_{h,j}^A(t) &= \sum_{x \in [x_j, x_{j+1})} \delta_{h,j}^A(x,t) \\
 y_{h,j}^B(t) &= \sum_{x \in [x_j, x_{j+1})} \delta_{h,j}^B(x,t) \\
 y_{h,j}^C(t) &= \sum_{x \in [x_j, x_{j+1})} \delta_{h,j}^C(x,t) \\
 y_{h,j}^{RC}(t) &= \sum_{x \in [x_j, x_{j+1})} \delta_{h,j}^{RC}(x,t)
 \end{aligned} \tag{13}$$

386 Also, to estimate density of B and C squats $d_{h,j}^{BC}(x,t)$, a window is defined around the coordinate x (in this
 387 paper, the window is 50 m in track length). The function $d_{h,j}^{BC}(x,t)$ equals the number of squats B or C in the
 388 moving window $[x - 0.025, x + 0.025]$. The KPI density for partition j , instant t , and scenario h can be
 389 defined as the area of the density function as follows:

$$390 \quad y_{h,j}^{dBC}(t) = \frac{\sum_{x \in [x_j, x_{j+1}]} d_h^{BC}(x,t)}{x_{j+1} - x_j} \quad (14)$$

391 Let's define a vector containing all the KPIs called $y_{h,j}(t)$ for partition j , instant t , and scenario h :

$$392 \quad y_{h,j}(t) = [y_{h,j}^A(t), y_{h,j}^B(t), y_{h,j}^C(t), y_{h,j}^{RC}(t), y_{h,j}^{dBC}(t)]^T \quad (15)$$

393 where $y_{h,j}^A(t)$, $y_{h,j}^B(t)$, $y_{h,j}^C(t)$, $y_{h,j}^{RC}(t)$ and $y_{h,j}^{dBC}(t)$ are the number of A squats, B squats, C squats, RC
 394 squat and the density of B squats C squats, respectively. Due to the large number of KPI's obtained in terms
 395 of all the growth scenarios and predictions over time, we propose two simple steps to include the effect of
 396 the trajectories of the KPIs into one global KPI:

397 Step 1: First, transform the vector $y_{h,j}(t)$ for each partition j , scenario h and instant t , into a single

398 KPI using a fuzzy expert system $y_{h,j}^M(t) = f_{\text{Mamdani}}(y_{h,j}^A(t), y_{h,j}^B(t), y_{h,j}^C(t), y_{h,j}^{RC}(t), y_{h,j}^{dBC}(t))$.

399 Step 2: Then, aggregate the single KPI over the set of scenarios and over the prediction horizon, for

400 each partition j . This results into a single global KPI for the current instant k , $J_j^{Rail}(k)$:

$$401 \quad J_j^{Rail}(k) = f_{\text{aggregate}}(y_{h_1,j}^M(k), \dots, y_{h_1,j}^M(k + N_P), \dots, y_{h_H,j}^M(k), \dots, y_{h_H,j}^M(k + N_P)) \quad (16)$$

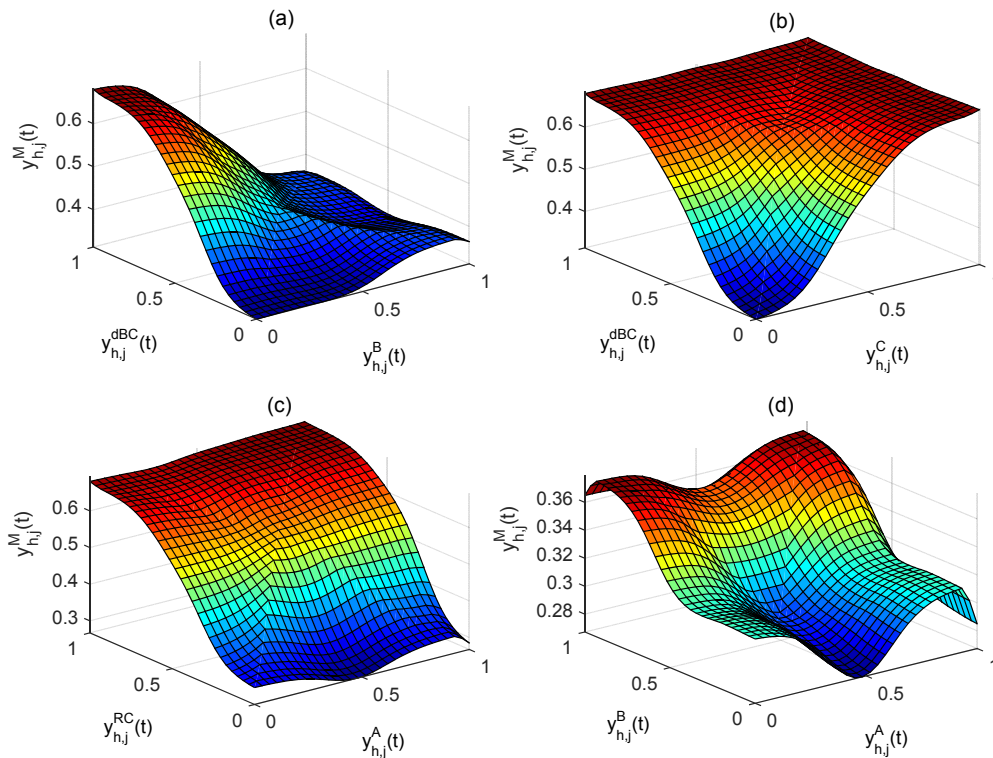
402 **Mamdani fuzzy KPI**

403 For Step 1, a Mamdani fuzzy expert system is used to calculate a single KPI (Mamdani and Assilian 1975).
 404 Even though the Mamdani fuzzy system approach was proposed more than 40 years ago, it is still popular
 405 because of its simplicity and interpretability (Camastra et al. 2015; Rezaei et al. 2015; Ozgur 2013). In this
 406 case, 32 fuzzy if-then rules are generated. The aim is to assign membership degree to each KPI to represent
 407 the contribution of each KPI in the rail health condition:

$$408 \quad \text{If } y_{h,j}^A(t) \text{ is } A_1^r \text{ and } y_{h,j}^B(t) \text{ is } A_2^r \text{ and } y_{h,j}^C(t) \text{ is } A_3^r \text{ and } y_{h,j}^{RC}(t) \text{ is } A_4^r \text{ and } y_{h,j}^{dBC}(t) \text{ is } A_5^r \\ \text{then } y_{h,j}^M(t) \text{ is } G^r$$

409 where A_1^r , A_2^r , A_3^r , A_4^r , A_5^r and G^r are the membership functions for rule r and $y_{h,j}^M(t)$ is the output
 410 Mamdani KPI. The KPIs are first normalized, then Gaussian membership functions are used to fuzzify the KPIs.
 411 Also, to defuzzify, centre of gravity method is applied in order to obtain crisp value at the end. Furthermore,
 412 relying on the fuzzy rules, interdependency of KPIs and Mamdani KPI are captured as shown in Figure 8. In
 413 this figure, it is presented how Mamdani KPI models the influence in the health of the track of two KPIs,
 414 varying from fully healthy (equals to zero) to completely unhealthy (equals to one), while all the other KPIs
 415 are assumed to be fully healthy (equals to zero). Four plots are presented. In Figure 8(a), a higher value for
 416 the BC density is much relevant than the contribution of the number of B squat. In Figure 8(b), a high number
 417 of C squats makes the most significant impact on the rail health condition. The rail condition will get highly
 418 unhealthy with high values of either density of the BC squats or number of C squat. In Figure 8(c), a high
 419 number of RC squats will influence much strongly on the health condition than the number of A squats. In
 420 the last plot, Figure 8(d), a high number of A squats or B squats will not have strong influence in the short
 421 term (the condition moves between the values 0.28 to 0.37). However, the number of B squats effects more
 422 negatively the rail health condition than the number of A squats. In Figure 8, appears the intuitive fact that
 423 rail condition gets worse with the increasing number of squat from A , B , C to RC .

424



425

426

Figure 8: Interdependency of KPIs over Mamdani KPI, $y_{h,j}^M(t)$.

427 In general, number of A squats will not have significant impact on the current rail health condition. However
 428 in the long term, if not ground, A squats will evolve into severe defects. In order to capture this and other
 429 dynamic effects, the prediction model is used, and the global KPI is calculated over time and under different
 430 scenarios.

431

432 **c. FUZZY GLOBAL KPI**

433 Relying on defined Mandani KPIs $y_{h,j}^M(t)$, a fuzzy global indicator is calculated to give a KPI over growth
 434 scenarios in partition j :

$$J_j^{Rail}(k) = \frac{\sum_{h \in \{h_1, h_2, h_3\}} \sum_{t=k}^{k+N_p} w_h \cdot w_t \cdot y_{h,j}^M(t)}{\sum_{h \in \{h_1, h_2, h_3\}} \sum_{t=k}^{k+N_p} w_h \cdot w_t} \quad (17)$$

where $J_j^{Rail}(k)$ is fuzzy global indicator, w_h is growth weight per scenario and w_t is a weight exponentially showing time effect on the KPIs. In this way, we aggregate different KPIs into a single one, that captures together stochasticities and evolution over time.

NUMERICAL RESULTS

a. FUZZY CONFIDENCE INTERVAL

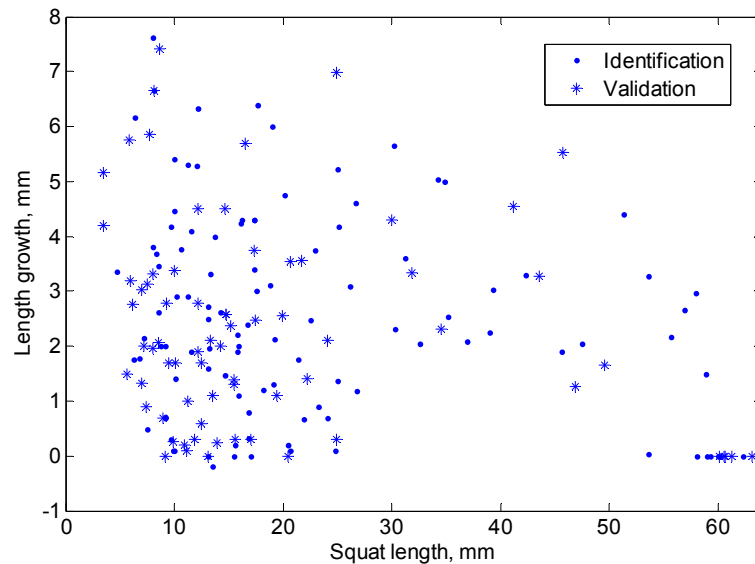
This section summarizes the simulation results to predict the squats length. A data set of squat lengths collected from different track visits are used to evaluate performance of squat growth model. Identification data and validation data for the interval fuzzy TS model are selected randomly, using 60% of the data for identification and 40% for validation (see Figure 9).

To optimize number of clusters, models from two to ten clusters are tested. For each number of cluster, the root mean square (RMS) of the prediction error is used to determine the best model. During the training, tuning parameters of the confidence interval fuzzy model are considered the same for the lower and upper fuzzy bounds. The idea is to obtain optimum parameter α , that results into a minimum number of data points outside the band whereas the band is as narrow as possible. Figure 10(a) depicts the Pareto front of the normalized area of the band versus the normalized number of data points outside the band ranging α from 0 to 40. Figure 10(b) shows how α behaves in terms of area of the band. As shown in the Figure 10(b), the area will reach maximum value if α equals to 32.

In reality, the variance of the worst case scenario is much larger than the best case scenario; thus the assumption of a fixed α must be relaxed. Using full trajectories of different squats, ad-hoc α^{h_1} and α^{h_3}

457 were obtained to better fit the dynamics. The use of interval fuzzy model for prediction is presented in Figure
458 12, with a selected $\alpha=1.5$ from the Pareto front, and modified parameters $\alpha^{h_1} = 0.32 \cdot \alpha$, and
459 $\alpha^{h_3} = 1.7 \cdot \alpha$. The squat length starts from a small defect in 8 mm to a severe squat in 60 mm. An important
460 characteristic is when the predictive model reaches the highest bound 60 mm. This happens for squats of 48
461 mm for the one-step ahead prediction (within 6 months), and it will happen for squats of 18 mm in the case
462 of four-step ahead prediction (within 24 months). For testing purposes, we have evaluated this model with
463 another data set of the trajectories presented in Li et al. (2010). All of them are contained within the interval
464 model.

465

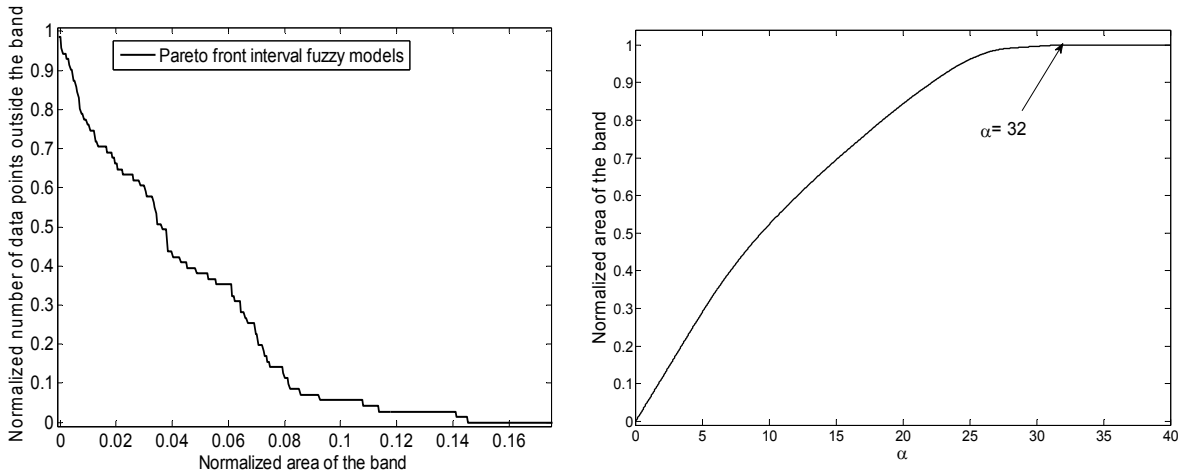


466

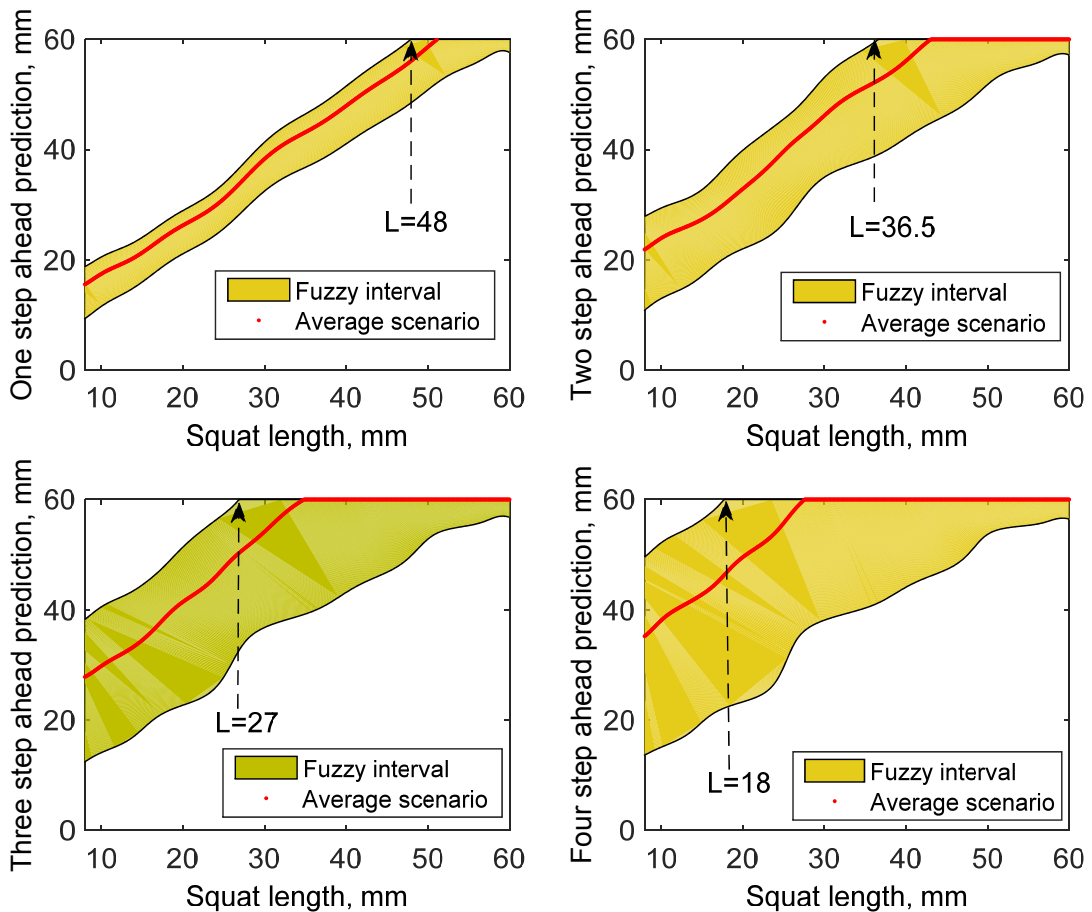
467

Figure 9: Validation and identification data for the squats length.

468



469
 470
 471
 Figure 10: (a) pareto front of number of data point outside v.s area of the band. (b) area of the band over α .



472
 473
 Figure 11: Interval fuzzy model predictions, one, two, three and four steps-ahead.

474 **b. FUZZY GLOBAL KPI FOR TRACK HEALTH CONDITION**

475 The full track of the Meppel-Leeuwarden is used to show the proposed methodology. The Figure 12 shows a
 476 simple map of the track and the four partitions j_1, j_2, j_3 and j_4 . The partitions can be adapted according to the
 477 maintenance plans or other design considerations. The partitions in this paper, are all around 10 kilometres
 478 long, except the last one which is 15 kilometres long. Meppel is in kilometre at 105, Leeuwarden is at 150,
 479 the partitions are defined between the kilometres: $x_{j_1} = 105, x_{j_2} = 115, x_{j_3} = 125, x_{j_4} = 135$ and $x_{j_5} = 150$.

480

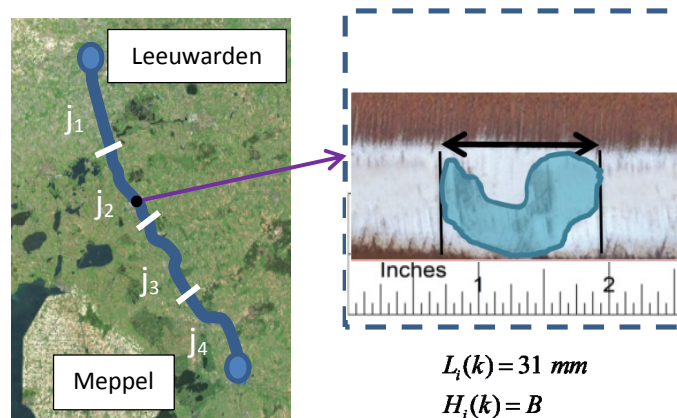
481

482

483

484

485

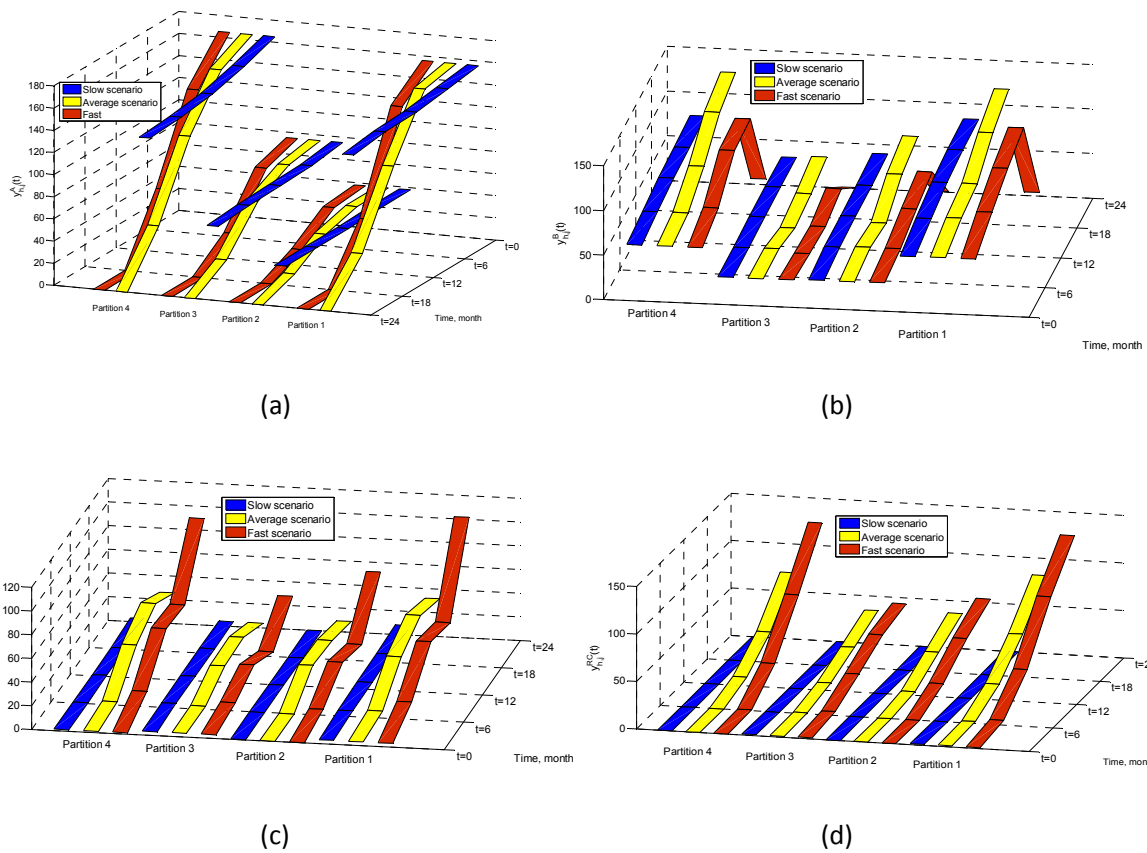


486 Figure 12: Schematic track map between two stations, Meppel and Groningen, divided into four partitions, $j_1,$
 487 $j_2, j_3,$ and j_4

488

489 Figure 13 shows the different KPIs squats number over four step-ahead prediction when no maintenance is
 490 performed. All the cases are calculated for the scenarios slow (in blue), average (in yellow) and fast (in red).
 491 In Figure 13(a), the number of A squat tends to get reduced over time, as they are becoming B squats. In
 492 Figure 13(b), the number of B squat increases because of the A squats becoming B squats, but after $t=12$, the
 493 number of B squat decreases as most of them are becoming C squat. When no corrective maintenance is

494 performed, it can be seen from Figure 13(c) that after $t=12$, huge number of C squats are in the track (worst
 495 case scenario), which is a very expensive situation as the only solution will be to replace the rails. In Figure
 496 13(d), it is possible to see the moment when operational risk locations start to appear, indicating that
 497 maintenance should be done before the worst case scenario indicates their appearance.
 498



499
 500

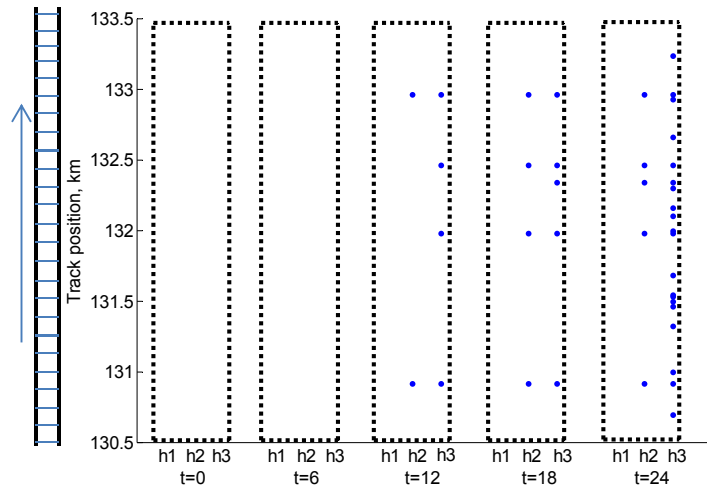
501
 502

503 Figure 13: Squat number KPIs for the slow, average and fast growth scenarios in the absence of maintenance
 504 operation, (a) number of A squat, (b) number of B squat, (c) number of C squat and (d) number of RC squats.

505

506 Figure 14a shows how potential risk squats will start to appear over time. Figure 14b shows the KPI related to
 507 density of B and C squats. As seen in Figure 14a, the first squats with high potential risk of derailment, RC
 508 squats, appear for the worst case scenario at $t=12$, in four kilometre positions $\{130.9, 132.0, 132.5, 133.0\}$.

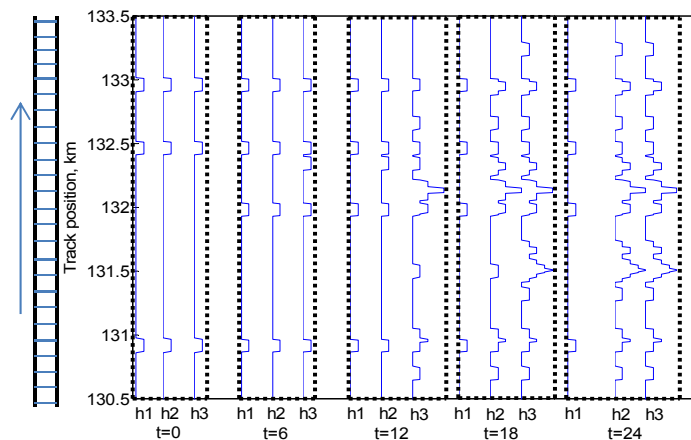
509 Three of those four locations were already detected at t=0 in Figure 14b, while all of them are already
 510 present in the B-C squat density signal at t=6 for all the scenarios. It means that within the first 12 month, the
 511 infrastructure manager is expected to take actions, to prevent risk of derailment.



512

513

(a)



514

515

516

517

518

519

(b)

520

521 Figure 14: For track position between 130.5 and 133.5km, predictions over 24 months and three scenarios
 522 for: (a) Potential risk locations, (b) B-C squats density.

523 The Figure 15 collects all the scenarios and the signals over the whole prediction horizon, to indicate a single
 524 global fuzzy KPI for each track partition. Three cases are considered, no maintenance, grinding at t=0, and
 525 local rail replacement at t=0 for each severe squat. Maintenance considerably can improve the rail health

526 condition, but to be fully efficient a combination of both grinding and replacement is necessary. After the
 527 maintenance operations, the condition is in the average condition range, where the potential risk of
 528 derailment is considerably lower during the prediction horizon. The following result allows the infrastructure
 529 manager to decide how to manage the rail in the future at each track partition. As in the case of the absence
 530 of maintenance operation, a cost of zero Euro with the clear consequence of the bad rail health condition. In
 531 the case of the grinding effect and the replacement effect, the results can be applied as an effective factor
 532 for cost analysis of the track maintenance plan.

533

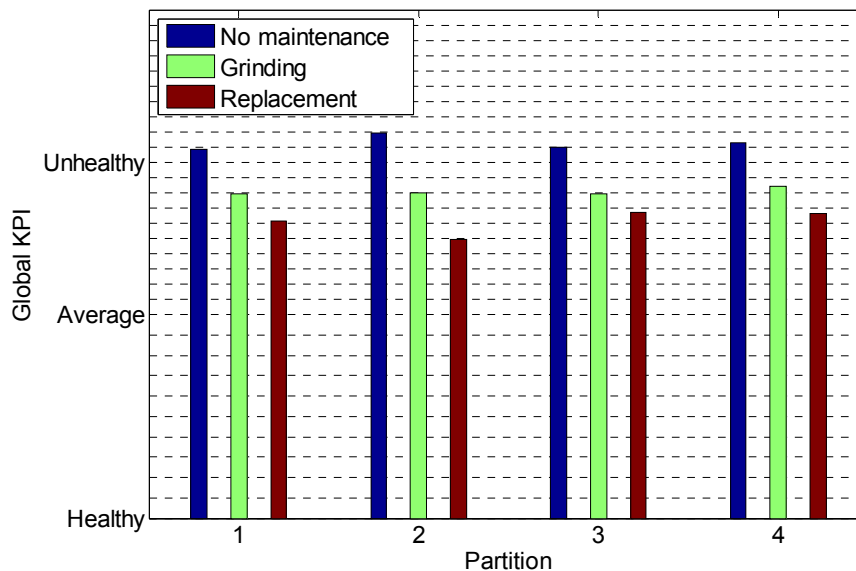


Figure 15: Fuzzy global KPIs

534

535

536

537 CONCLUSION AND FUTURE RESEARCH

538 In this paper a condition-based monitoring methodology is developed for a type of surface defect in the rail
 539 called "squats". This methodology is employed to construct an interval-based TS fuzzy prediction modelling
 540 in order to monitor the track condition over maintenance time horizon per track partition.

541 The idea of using fuzzy interval is to capture all the possible growth scenarios. Based on the interval fuzzy
 542 models for squats, a condition-based methodology for railway tracks is proposed using different KPIs defined

543 in a track-partition level, allowing the grouping of defects located in a given track partition. In the
544 methodology, number and density of squats are considered over a prediction horizon under three different
545 scenarios, slow, average and fast growth. Then, to facilitate visualization of the rail health condition and to
546 ease the maintenance decision process, we propose a fuzzy global KPI based on fuzzy rules for each partition,
547 that combine the different KPIs over prediction horizon and scenarios. Hence, the proposed methodology
548 adds value by defining fuzzy global KPIs which are predictable over time to facilitate maintenance decision
549 making of the rail. As an example, the KPIs obtained are presented for the track Meppel-Leeuwarden.

550 As a further research, the study will be oriented into an optimization-based methodology to reduce life cycle
551 costs effectively and to fit the methodology much closely to the real-life maintenance operations. The use of
552 new predictive and robust KPIs defined for different parties will be considered, including infrastructure
553 manager, rolling stock manager, contractors and users.

554

555

ACKNOWLEDGEMENTS

556 Research sponsored by the NWO/ProRail project "Multiparty risk management and key performance
557 indicator design at the whole system level (PYRAMIDS)", project 438-12-300, which is partly financed by the
558 Netherlands Organisation for Scientific Research (NWO) and by the Collaborative Project H2020-MG-2015-
559 2015 GA-398 636237b Needs Tailored Interoperable Railway - NeTIRail-INFRA. We also thank Meysam
560 Naeimi for the discussions about the effect and modelling of grinding.

561

562 REFERENCES

563 Åhrén, T., and Parida, A. (2009). "Maintenance performance indicators (MPIs) for benchmarking the railway
564 infrastructure: a case study." *Benchmark. Int. J.*, 16(2), 247-258.

Please cite as: A. Jamshidi, A. Núñez, R. Dollevoet, and Z. Li, "Robust and predictive fuzzy key performance indicators for condition-based treatment of squats in railway infrastructures". *Journal of Infrastructure Systems*, Volume 23, Issue 3, September 2017.

DOI: 10.1061/(ASCE)IS.1943-555X.0000357

Find published version at www.ascelibrary.org

- 565 Andrade, A. R., and Teixeira, P. F. (2011). "Uncertainty in Rail-Track Geometry Degradation: Lisbon-Oporto Line Case
566 Study." *J. Transp. Eng.*, 10.1061/(ASCE)TE.1943-5436.0000206, 193-200.
- 567 Andrade, A. R., and Teixeira, P. F. (2012). "A Bayesian model to assess rail track geometry degradation through its life-
568 cycle." *Res. Transport. Econ.*, 36(1), 1-8.
- 569 Andrews, J. (2012). "A modelling approach to railway track asset management. *Proceedings of the Institution of*
570 *Mechanical Engineers.*" *P. I. Mech. Eng. F-J. Rai.*, 227(1), 56-73.
- 571 Burstow, M.C., Watson, A.S., and Beagles, M. (2002). "Application of the whole life rail model to control rolling contact
572 fatigue." *Proc., Int. Conf. of Railway Engineering*, London.
- 573 Camastra, F., Ciaramella, A., Giovannelli, V., Lener, M., Rastelli, V., Staiano, A., and Starace, A. (2015). "A fuzzy decision
574 system for genetically modified plant environmental risk assessment using Mamdani inference." *Expert Syst.*
575 *Appl.*, 42(3), 1710-1716.
- 576 Guler, H. (2014). "Prediction of railway track geometry deterioration using artificial neural networks: a case study for
577 Turkish state railways." *Struct. Infrastruct. E.*, 10(5), 614-626.
- 578 Khatri, K., Vairavamoorthy, K., and Akinyemi, E. (2011). "Framework for Computing a Performance Index for Urban
579 Infrastructure Systems Using a Fuzzy Set Approach." *J. Infrastruct. Syst.*, 10.1061/(ASCE)IS.1943-555X.0000062, 163-175.
- 580 Kisi, O. (2013). "Applicability of Mamdani and Sugeno fuzzy genetic approaches for modeling reference
581 evapotranspiration." *J. Hydrol.*, 504, 160-170.
- 582 Lewis, R., and Olofsson, U. (Eds.). (2009). *Wheel-rail interface handbook*, Woodhead publishing limited, Cambridge, U.K.
- 583 Li, Z., Dollevoet, R., Molodova, M., Zhao, X. (2011). "Squat growth—Some observations and the validation of numerical
584 predictions." *Wear*, 271(1–2), 148-157.
- 585 Li, Z., Molodova, M., Núñez, A., and Dollevoet, R. (2015). "Improvements in axle box acceleration measurements for the
586 detection of light squats in railway infrastructure." *IEEE T. Ind. Electron.*, 62(7), 4385-4397.

Please cite as: A. Jamshidi, A. Núñez, R. Dollevoet, and Z. Li, "Robust and predictive fuzzy key performance indicators for condition-based treatment of squats in railway infrastructures". *Journal of Infrastructure Systems*, Volume 23, Issue 3, September 2017.

DOI: 10.1061/(ASCE)IS.1943-555X.0000357

Find published version at www.ascelibrary.org

- 587 Li, Z., Molodova, M., Zhao, X., and Dollevoet, R. (2010). "Squat treatment by way of minimum action based on early
588 detection to reduce life cycle costs." *Proc., of the Joint Rail Conf., Urbana Illinois*.
- 589 Li, Z., Zhao, X., Esveld, C., Dollevoet, R., and Molodova, M. (2008). "An investigation into the causes of squats—
590 correlation analysis and numerical modeling." *Wear*, 265(9), 1349-1355.
- 591 Magel, E.E., and Kalousek, J. (2002). "The application of contact mechanics to rail profile design and rail
592 grinding." *Wear* 253(1), 308-316.
- 593 Mamdani, E.H., and Assilian, S. (1975). "An experiment in linguistic synthesis with a fuzzy logic controller." *Int. J. Man.*
594 *Mach. Stud.*, 7(1), 1-13.
- 595 Mohammad, R., Mostafa, A., Abbas, M., and Farouq, H. M. (2015). "Prediction of representative deformation modulus
596 of longwall panel roof rock strata using Mamdani fuzzy system." *Int. J. of Mining Science and Technology*, 25(1), 23-30.
- 597 Molodova, M., Li, Z., Núñez, A., and Dollevoet, R. (2014). "Automatic detection of squats in railway infrastructure." *IEEE*
598 *T. Intell. Transp.*, 15(5), 1980-1990.
- 599 Molodova, M., Li, Z., Núñez, A., and Dollevoet, R. (2015). "Parameter study of the axle box acceleration at squats." *P. I.*
600 *Mech. Eng. F-J. Raj*, 229(8), 841-851.
- 601 Nathanail, E. (2014). "Framework for Monitoring and Assessing Performance Quality of Railway Network Infrastructure:
602 Hellenic Railways Case Study." *J. Infrastruct. Syst.*, 10.1061/(ASCE)IS.1943-555X.0000198, 04014019.
- 603 Nuñez, A., and De Schutter, B. (2012). "Distributed identification of fuzzy confidence intervals for traffic
604 measurements." *Proc., 51st Annual Conf. on Decision and Control (CDC), Hawaii*, 6995–7000.
- 605 Parida, A., and Chattopadhyay, G. (2007). "Development of a multi-criteria hierarchical framework for maintenance
606 performance measurement (MPM)." *J. Qual. Mainten. Eng.*, 13(3), 241-258.
- 607 Patra, A. P., Söderholm, P., and Kumar, U. (2009). "Uncertainty estimation in railway track life-cycle cost: a case study
608 from Swedish National Rail Administration." *P. I. Mech. Eng. F-J. Raj*, 223(3), 285-293.

Please cite as: A. Jamshidi, A. Núñez, R. Dollevoet, and Z. Li, "Robust and predictive fuzzy key performance indicators for condition-based treatment of squats in railway infrastructures". *Journal of Infrastructure Systems*, Volume 23, Issue 3, September 2017.

DOI: 10.1061/(ASCE)IS.1943-555X.0000357

Find published version at www.ascelibrary.org

- 609 Rail Damages, (2001). "The Blue Book of RailTrack." U.K.
- 610 Rockafellar, R., and Royset, J. (2015). "Engineering Decisions under Risk Averseness." *ASCE-ASME J. Risk Uncertainty Eng. Syst., Part A: Civ. Eng.*, 1(2).
- 611
- 612 Sadeghi, J., and Askarinejad, H. (2010). "Development of improved railway track degradation models." *Struct. Infrastruct. E.*, 6(6), 675-688.
- 613
- 614 Sadiq, R., Rajani, B., and Kleiner, Y. (2004). "Fuzzy-Based Method to Evaluate Soil Corrosivity for Prediction of Water Main Deterioration." *J. Infrastruct. Syst.*, 10.1061/(ASCE)1076-0342(2004)10:4(149), 149-156.
- 615
- 616 Sáez, D., Avila, F., Olivares, D., Cañizares, C., and Marin, L. (2015). "Fuzzy prediction interval models for forecasting renewable resources and loads in microgrids." *IEEE Trans. Smart Grid*, 6(2), 548-556.
- 617
- 618 Sandström, J., and Ekberg, A. (2009). "Predicting crack growth and risks of rail breaks due to wheel flat impacts in heavy haul operations." *P. I. Mech. Eng. F-J. Rai*, 223(2), 153-161.
- 619
- 620 Schafer, D., and Barkan, C.P. (2008). "A prediction model for broken rails and an analysis of their economic impact." *Proc., of the AREMA*, Salt Lake, UT.
- 621
- 622 Senouci, A., El-Abbasy, M., and Zayed, T. (2014). "Fuzzy-Based Model for Predicting Failure of Oil Pipelines." *J. Infrastruct. Syst.*, 10.1061/(ASCE)IS.1943-555X.0000181, 04014018.
- 623
- 624 Škrjanc, I. (2011). "Fuzzy confidence interval for pH titration curve." *Appl. Math. Model*, 35(8), 4083-4090.
- 625
- 626 Škrjanc, I., Blažič, S., and Agamennoni, O. (2004). "Identification of dynamical systems with a robust interval fuzzy model." *Automatica*, 41(2), 327-332. DOI: 10.1016/j.automatica.2004.09.010
- 627
- 628 Smulders, J. (2003). "Management and research tackle rolling contact fatigue." *Railway Gazette Int.*, 158(7), 439-442
- 629
- 628 Stenström, C., Norrbin, P., Parida, A., and Kumar, U. (2015). "Preventive and corrective maintenance–cost comparison and cost–benefit analysis." *Struct. Infrastruct. E.*, 1-15.

Please cite as: A. Jamshidi, A. Núñez, R. Dollevoet, and Z. Li, "Robust and predictive fuzzy key performance indicators for condition-based treatment of squats in railway infrastructures". *Journal of Infrastructure Systems*, Volume 23, Issue 3, September 2017.

DOI: 10.1061/(ASCE)IS.1943-555X.0000357

Find published version at www.ascelibrary.org

- 630 Stenström, C., Parida, A., Lundberg, J., and Kumar, U. (2015). "Development of an integrity index for benchmarking and
631 monitoring rail infrastructure: application of composite indicators." *Int. J. Rail Transp.*, 3(2)-61-80.
- 632 UIC Code, (2002). "Rail Defects." *Int. Union of Railways, 4th ed.*, Paris, France.
- 633 Vale, C., and Lurdes, S. M. (2013). "Stochastic model for the geometrical rail track degradation process in the
634 Portuguese railway Northern Line." *Reliab. Eng. Syst. Safe*, 116, 91-98.
- 635 Wang, K. and Liu, F. (1997). "Fuzzy Set-Based and Performance-Oriented Pavement Network Optimization System." *J.*
636 *Infrastruct. Syst.*, 10.1061/(ASCE)1076-0342(1997)3:4(154), 154-159.
- 637 Weston, P., Roberts, C., Yeo, G., and Stewart, E. (2015). "Perspectives on railway track geometry condition monitoring
638 from in-service railway vehicles." *Vehicle Syst. Dyn.*, 57(7), 1063-1091.
- 639 Xu, J., Tu, Y., and Lei, X. (2014). "Applying Multiobjective Bilevel Optimization under Fuzzy Random Environment to
640 Traffic Assignment Problem: Case Study of a Large-Scale Construction Project." *J. Infrastruct. Syst.*,
641 10.1061/(ASCE)IS.1943-555X.0000147, 05014003.
- 642 Zoeteman, A. (2001). "Life cycle cost analysis for managing rail infrastructure." *E.J.T.I.R.*, 1(4), 391 - 413.
- 643 Zoeteman, A. and van Meer, G. (2006). "A yardstick for condition based and differential planning of track and turnout
644 renewal: A major step towards full decision support." *Proc., 7th World Cong. on Railway Research (WCRR2006)*,
645 Montreal.
- 646 Zoeteman, A., Dollevoet, R., and Li, Z. (2014). "Dutch research results on wheel/rail interface management: 2001-2013
647 and beyond." *Proceedings of the Institution of Mechanical Engineers, P. I. Mech. Eng. F-J. Rai*, 228(6), 642-651.